Hydrogenated Amorphous Silicon Sensors based on Thin Film on ASIC technology

M. Despeisse, D. Moraes, G. Anelli, P. Jarron, J. Kaplon, R. Rusack, S. Saramad and N. Wyrsch

Abstract – **The performance and limitations of a novel detector technology based on the deposition of a thin-film sensor on top of processed integrated circuits have been studied. Hydrogenated amorphous silicon (a-Si:H) films have been deposited on top of CMOS circuits developed for these studies and the resulting "Thin-Film on ASIC" (TFA) detectors are presented. The leakage current of the a-Si:H sensor at high reverse biases turns out to be an important parameter limiting the performance of a TFA detector. Its detailed study and the pixel segmentation of the detector are presented. High internal electric fields (in the order of 10^4-10^5 V/cm) can be built in the a-Si:H sensor and overcome the low mobility of electrons and holes in a-Si:H. Signal induction by generated carrier motion and speed in the a-Si:H sensor have been studied with a 660 nm pulsed laser on a TFA detector based on an ASIC integrating 5 ns peaking time pre-amplifiers. The measurement set-up also permits to study the depletion of the sensor and results are presented. Finally, direct detection of 5.9 keV X-rays with TFA detectors based on an ASIC integrating low noise pre-amplifiers (27 e^- r.m.s) are shown.**

I. Introduction

HIGH resistivity crystalline silicon (c-Si) is now a well established detector technology and is widely used in tracking applications in several High Energy Physics experiments. We have investigated an alternative solid state detector technology based on the deposition of a hydrogenated amorphous silicon sensor directly on top of the readout integrated circuit. This technology, called Thin-Film on ASIC (TFA) ([1], [2]), potentially offers radiation hard alternatives to silicon devices. The vertical integration of a thin film sensor on the ASIC eliminates the need for bump bonding and enables a level of integration comparable to monolithic pixels while having the advantages of the hybrid pixel approach.

Hydrogenated amorphous silicon (a-Si:H) is used as sensing device. This material has been studied in the past 30 years and is well known nowadays though it still presents many controversial issues. a-Si:H is widely industrialized in thin films (< 1 µm) for solar cells and various sensitive imaging devices. Radiation hardness has been studied in the context of testing solar cells for space applications. It has been shown that proton, neutron and electron irradiation ([3]-[5]) or photon irradiation (involving the Staebler Wronski effect [4], [6]) all lead to a creation of metastable deep defects that can be annealed out, resulting in a good radiation hardness of the material in comparison to c-Si. a-Si:H can be deposited at low cost and on large areas at temperatures below 250 °C which are compatible with processed integrated circuits. TFA detector using a-Si:H as a detecting device is then an attractive solution for a radiation hard pixel detector.

However, for particle detection, thicker a-Si:H layers and full depletion of the sensor are needed to provide adequate signal over noise ratio [5]. A first technological challenge consists in the deposition of a-Si:H layers with thickness higher than 30 µm on ASIC with a minimal defect density to allow full depletion of the sensor and minimal leakage currents for the high reverse biases needed for the sensor depletion [7]. The voltage V_d needed to deplete an a-Si:H sensor of thickness d (in µm) can be estimated by considering a density of ionized dangling bonds of the material $N_{db}^* \sim 6\times10^{14}$ cm^{-3} and $V_d \sim 0.45\times d^2$ [1]. Sensors with a thickness higher than 50 µm are then difficult to grow and would moreover necessitate reverse voltages of about 1.1 kV for full depletion. Sensors with thicknesses up to 36 µm have then been deposited in our studies, which can be considered thick in comparison to standard a-Si:H opto-electronic devices but thin in comparison to standard crystalline silicon detectors with thicknesses higher than 150 µm.

Different groups have performed characterization of a-Si:H sensors deposited on a glass substrate and demonstrated that the signal created by a particle in the a-Si:H sensor is small [5], [8], [9] (Minimum Ionizing Particles are expected to create few hundred of electrons in 20 µm thick sensors). One of the resulting challenges in the development of this technology is to design low noise pre-amplifiers able to readout the small signal induced by a particle going through the thin a-Si:H sensor. The potential of a pixel sensor based on this novel technology has been investigated together with the design of adapted integrated circuits and together with the characterization of the a-Si:H electrical properties, i.e. signal induction speed, detection characteristics and radiation hardness.

II. TFA Sensors Developed

The a-Si:H sensor is built on top of the ASIC by consecutive depositions of n-doped, intrinsic and p-doped (n-i-p) a-Si:H films. Depositions have been performed at the Institute of Micro-technology of Neuchâtel (IMT) by Very High Frequency Plasma Enhanced Chemical Vapor Deposition at 70 MHz and 200 °C using an hydrogen dilution of Silane, and a deposition rate of 15.6 Å/s was obtained [7]. The n-i-p diodes were deposited on different ASICs developed

Manuscript received November 10, 2005.

M. Despeisse, D. Moraes, G. Anelli, P. Jarron, J. Kaplon and S. Saramad are with the European Organization for Nuclear Research (CERN), CH-1211 Geneva 23, Switzerland (telephone: +41-22-767-21-30, e-mail: matthieu.despeisse@cern.ch).

M. Despeisse and R. Rusack are with the school of physics and astronomy of the University of Minnesota, 116 Church Street SE, Minneapolis, MN 55455.

N. Wyrsch is with the Institute of Microtechnology, IMT, Breguet 2, CH-2000 Neuchatel, Switzerland.

for our studies. The n-layer and p-layer have high defect density resulting in the recombination of charge carriers generated in these layers. The doped layer thus only permit the application of reverse voltages on the i-layer and are therefore deposited very thin (≤30 nm). The diode thickness is then equivalent to the i-layer thickness. The bottom contacts are defined by metal structures integrated in the ASIC and designed in the last metal layer of the technology. The different metal structures integrated in the ASIC are inter-connected through the n-layer. In order to avoid a patterning of this layer, it is specially designed with low conductivity providing pixel isolation. A Transparent Conductive Oxide (TCO) layer is deposited on the p-layer and defines the global top electrode; this TCO layer is usually made of ITO (Indium Tin Oxide). A schematic cross section of a TFA detector is presented in Fig 1.

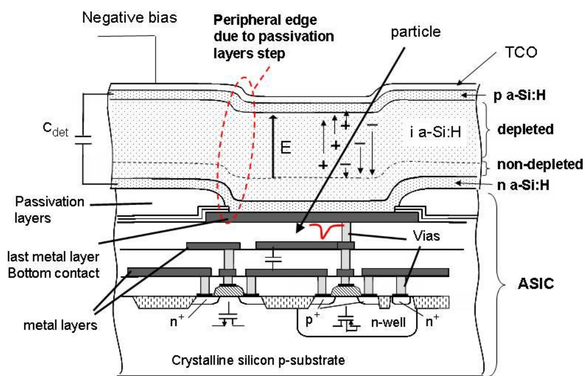

Fig. 1. Schematic cross section of a TFA detector based on the deposition of n-i-p a-Si:H layers and TCO electrode on top of an ASIC with 3 levels of metal.

a-Si:H sensors were deposited on 3 different ASICs (AFP, MACROPAD and aSiHtest) each designed in a CMOS 0.25 µm technology. The 3 integrated circuits contain different integrated metal structures and pre-amplifiers optimized for different speed and noise performance.

The AFP chip contains 32 68 µm × 94 µm metal pads each connected to an integrated Active Feedback Pre-amplifier which has a 5 ns peaking time for an Equivalent Noise Charge (ENC) of about 400 e- rms [10].

The MACROPAD circuit consists of 48 octagonal pads with about 140 µm width and 380 µm pitch, each pad being connected to a transimpedance amplifier followed by a shaper stage. The circuit has a peaking time of about 160 ns, and an ENC of 27 e^- rms [11].

The aSiHtest chip has been designed as a test chip to characterize the TFA technology. Different metal structures are integrated in the center of the chip and define the detector active area (Fig. 2). 21 structures with areas of 18638 μm^2 or 167747 μm^2 and with different shapes are integrated to study the leakage current of the a-Si:H sensor and the detector pixel segmentation. Each structure is connected to current mirror stages which provide a current gain of 10^2 to 10^5. Final process steps during the fabrication of the ASIC consist in depositing passivation layers on top of the chip and in opening windows in these layers on top of each metal pad to permit external access. Openings are normally performed inside the metal pad so that the 5 µm thick passivation layers induce unevenness of the circuit surface and of the TFA detector (Fig 1). The aSiHtest chip integrates metal structures for which the openings were performed outside the metal structures in order to study the impact of the passivation layer step on the detector performance.

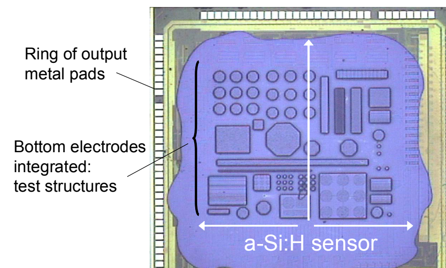

Fig. 2. Picture of a TFA detector based on a 20 µm thick n-i-p a-Si:H diode deposited on top of an aSiHtest integrated circuit.

24 other metal structures integrated in the center of the circuit are each connected either to a fast pre-amplifier with 5 ns peaking time for an ENC of 160 e^- rms or to a low noise pre-amplifier with a 25 ns peaking time for an ENC of 70 e^- rms. The structures are octagons with an area of 18638 μm^2 and 2070 μm^2 and strips with an area of 1864 μm^2 for a pitch varying from 23 µm to 3 µm. The strip structures have been integrated in order to study the potential of the TFA technology for high resolution strip detectors.

III. EXPERIMENTAL RESULTS

A. Electrical characterization and pixel segmentation

Low dark reverse bias currents of the a-Si:H sensor are needed in order to be able to fully deplete the sensor and to have an adequate signal over noise ratio. The leakage current of thin (≤ 1 µm) n-i-p a-Si:H sensors has been shown to originate from thermal generation in the intrinsic layer [12]. However, thicker layers are needed for particle detection. High reverse biases are required for full depletion of the sensor resulting in elevated electric field (> 10^4 V/cm) in the depleted region, and in increased leakage currents [13]. Results obtained on thick a-Si:H sensors (up to 32.6 µm) deposited on a glass substrate are presented in [2]. TFA detectors developed on a MACROPAD and on an AFP chip showed leakage current up to 3 orders of magnitude higher than for similar sensors deposited on a glass substrate ([11], [14]), showing a strong increase of the a-Si:H sensor leakage current linked to its deposition on an ASIC.

The thermal generation of charges is enhanced by the electric field by Poole-Frenkel mechanisms [13], so that local elevated fields in a pixel might create higher leakage currents. The pixel active area of a detector made of a 32.6 µm thick diode and of an AFP chip has been studied using a Scanning Electron Microscope (SEM). A 20 keV electron beam scans a pixel and the signal induced on the bottom electrode is amplified by the integrated pre-amplifier and fed back to the

SEM operating system. Electron Beam Induced Current (EBIC) images are built with contrast proportional to the amplitude of the induced signal, which depends on the depleted thickness, on the internal electric field which modifies the drift velocities of carriers generated and on the weighting field. The SEM picture and EBIC image obtained on a pixel are presented in Fig. 3, for a 260 V reverse bias applied to the sensor.

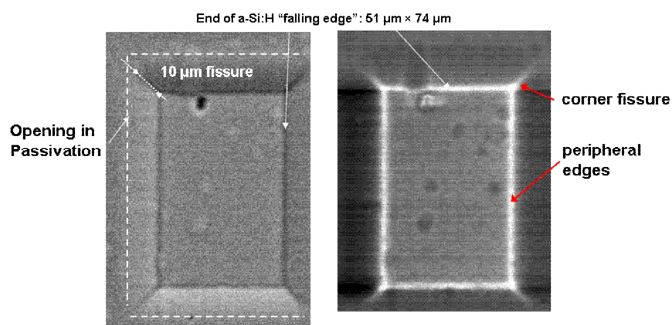

Fig. 3. EBIC study of a pixel of a TFA detector made of a 32 µm thick a-Si:H sensor on top of an AFP chip. Left: SEM picture showing geometrical effects caused by the passivation layer steps. Right: EBIC image. White zones correspond to higher induced current.

The SEM picture shows a peripheral edge and some fissures at the corners of the pixel, caused by the unevenness of the ASIC surface as represented in Fig. 1. The EBIC image clearly shows the effect of this particular geometry on the detector electric field: higher EBIC currents are observed at the edges and corners, indicating higher electric fields at these regions which might cause the higher leakage currents.

The additional currents suggested by the EBIC measurements have been studied on different detectors based on the aSiHtest chip by measuring leakage currents on the different metal structures integrated. Tendencies measured on the different samples are illustrated by results obtained on a 20 µm thick sample (Fig. 4).

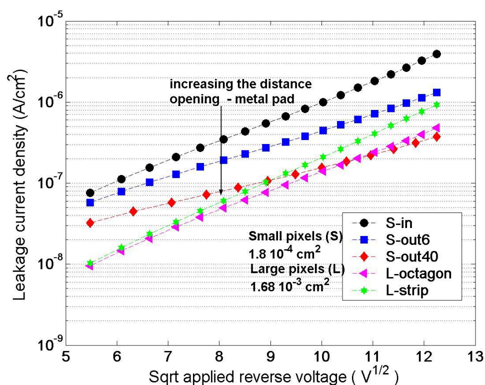

Fig. 4. Leakage current density measured on a TFA detector made of a 20 µm thick sensor on top of an aSiHtest chip. The sensor is not fully-depleted for the range of applied biases. L-octagon is an octagonal structure and L-strip a strip structure, both structures with an opening inside the metal pad and with an area of 1.68×10^{-3} cm^2. S-in, S-out6 and S-out40 are octagons with an area of 1.8×10^{-4} cm^2 and with passivation openings respectively inside the metal pad and outside, at 6 µm and at 40 µm from the metal pad edges.

The leakage current density of the different structures varies exponentially with the square root of the applied voltage. An octagon with an area of 1.8×10^{-4} cm^2 presents a current density a factor 6 lower than an octagon with an area 9 times smaller. This is a first indication of currents arising from the pixel edges and corners, as the ratio perimeter/area is higher for smaller structures, and as the pixel corners should not depend on the pixel size. A strip structure has a higher leakage current than an octagon because of a higher perimeter/area ratio (Fig. 4). These differences demonstrate a strong contribution to the TFA detector leakage current arising from the periphery and corners of a pixel.

Octagonal structures with openings in the passivation outside the metal pad are also integrated in the aSiHtest chip. A clear reduction of leakage current density is observed for these structures (Fig. 4), scaling with the distance of the opening location to the metal pad edges.

Opening the passivation layers outside the metal pad then leads to a reduction of the additional currents, as these currents contribute to the total leakage current of the pixel only after conduction through the low conductivity n-layer.

The mechanisms responsible of the elevated dark currents at high reverse biases have been studied by measuring the evolution of the current with temperature (Fig. 5).

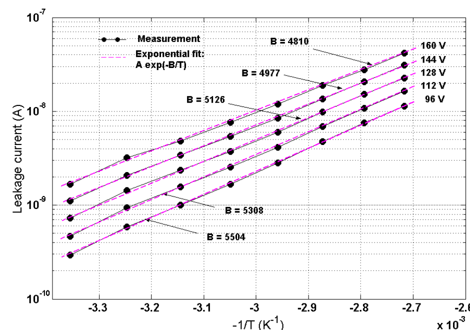

Fig 5. Evolution of leakage current with temperature measured on a 20 µm thick a-Si:H sensor on top of an aSiHtest circuit.

The leakage current induced by thermal generation enhanced by electric field by Poole-Frenkel mechanisms can be written as [13]:

$$I = I_0 \exp(-E_A / kT) \quad (1); \qquad E_A = E_G / 2 - \gamma\sqrt{E} \quad (2).$$

E_G is the material bandgap, E_A is the activation energy, i.e. the energy needed to activate ionisable defects and γ is the Poole-Frenkel constant. Experimental data are well fitted by equations (1) and (2) (Fig. 5), showing that the leakage current can be attributed to Poole-Frenkel reduction of the activation energy, enhancing the thermal generation of charges. The activation energies have been extracted for different structures and show similar results, thus demonstrating that additional currents arising from the pixel edges and corners are also mainly determined by this effect. The activation energy decreases for increasing applied voltage and is equal to 0.49 eV and 0.42 eV for 80 V and 160 V reverse biases.

B. *Signal induction and speed in TFA detectors*

The motion of charge carriers generated by radiation incident on an a-Si:H sensor induces a current on the sensor electrodes. The induced current speed is a crucial parameter of the detector performance and has been studied by measuring a TFA detector response to a 660 nm pulsed laser light. The laser pulse impinges on the top electrode and since 660 nm photons have a mean free path of 1 μm in a-Si:H, electron-hole pairs are generated close to the p-i interface of the sensor. Generated electrons drift down through the whole depleted thickness and generated holes drift on a short distance up to the p^+ layer where they are absorbed or recombine. The signal induced on the detector bottom electrode integrated in the ASIC is then mainly determined by the electron motion. The moving charges induce a signal proportional to the total charge, to the velocity of the charges and to the weighting field of the detector [15]. For under-depleted a-Si:H sensors, the non-depleted i-layer has a low conductivity ($\sigma < 10^{-10}$ S cm^{-1}), so that a current is induced only while the created charge packet is moving [15]. Tests with a 660 nm pulsed laser have been performed on a 32.6 μm thick sensor deposited on an AFP circuit. Pre-amplifier output signals measured for 3 ns FWHM pulses for different detector reverse biases are presented in Fig. 6.

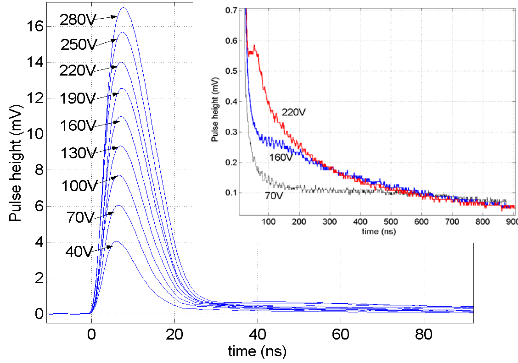

Fig 6. Response of a 20 μm thick a-Si:H sensor on top of an AFP circuit to a 3 ns FWHM 660 nm laser pulse for different detector biases. Fast decay of the output pulses correspond to the electron drift, long tail of signal correspond to hole drift.

The signal rise corresponds to the pre-amplifier peaking time (~ 5ns) and to the time of generation of charges, which corresponds to the laser pulse duration here of 3 ns. The peaks correspond to the signal induced by the electron packet moving in the high field region. The packet drifts under decaying electric field so that the induced signal then decreases. By increasing the detector reverse voltage, electric field and drift distance (given by the width of the depleted region) are increased resulting in global constant signal decay time of about 20 ns. Tails are observed in the output signals, varying with the electric field. Signal induced by holes as well as electron reemitted from deep traps causes this long tail. Hole transport is dispersive and hole mobility is field dependent [16] so that variations of the detector bias strongly impact the hole motion.

A simple model of the current induced by the electron motion has been developed considering an electric field linearly decaying from its maximum at the p-i interface down to the end of the depleted region where it is nil. Simplified expressions for the electric field, the depleted thickness d and the electron motion x(t) are presented in [1]. Electron transport is non-dispersive in a-Si:H at room temperature and its drift mobility μ_d is considered as constant, so that electrons created at the p-i interface will have a motion along the whole depleted thickness d defined by:

$$x(t) = d\left(1-\exp\left(-t/\tau_c\right)\right) \quad (3);$$

$$\tau_c = \varepsilon_0 \varepsilon_{aSi} / \left(q \mu_d N_{db}^{*}\right) \quad (4)$$

The electron induced signal time constant τ_c depends on the the inverse of the product drift mobility-density of ionized dangling bonds. The current created by electrons generated at the p-i interface and drifting in the decaying electric field can be expressed as:

$$I(t) = \begin{cases} \dfrac{-q\cdot N}{d_{tot}} \dfrac{d\cdot A\cdot t}{\tau_c \cdot t_1} & \text{for } t < t_1 \\ \dfrac{-q\cdot N}{d_{tot}} \dfrac{d\cdot A}{\tau_c} \exp\left(-\left(t-t_1\right)/\tau_c\right) & \text{for } t > t_1 \end{cases} \quad (5)$$

The factor A is equal to $2\tau_c/(2\tau_c + t_1)$ where t_1 is the duration of the laser pulse. d_{tot} is the sensor thickness ($1/d_{tot}$ is a simplified expression of the sensor weighting field) and q·N is the total charge moving.) Simulations of the pre-amplifier output response to input currents defined by equation (5) have been performed with HSPICE. Current signals rising in ~ 3 ns (corresponding to the laser pulse width) and then decaying as defined by equation (5) permit a very good between the simulated and measured AFP output response (Fig 7).

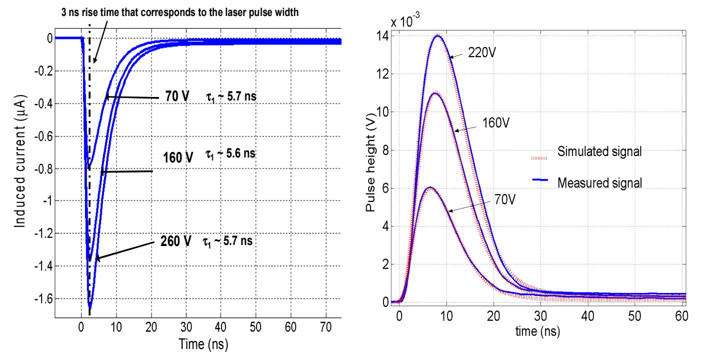

Fig 7. Left: Calculated currents created by electrons generated at the p-I interface during 3 ns and then drifting in the decreasing electric field. Right: simulation of the AFP output response to currents presented on left. A good fitting of the fast decay component is observed with measured signals.

The parameter τ_c can be extracted from these simulations and we obtained τ_c = 5.6 ns. The product $\mu_d \cdot N_{db}^{*}$ can also be extracted and is equal to 1.18×10^{15} $cm^{-1}V^{-1}s^{-1}$. For an expected value of N_{db}^{*} of 6×10^{14} cm^{-3} the electron mobility can be extracted and $\mu_d \sim 2$ $cm^2V^{-1}s^{-1}$, which is in agreement with

usual values of 1 to 5 2 $cm^2V^{-1}s^{-1}$ in a-Si:H. The high electric field inside the a-Si:H sensor (> 10^4 V/cm) leads to reasonable drift velocity of the electrons even though they have a low mobility, and signal induced by the electrons lasts for ~ 16.8 ns.

The signal tails are induced by the movement of holes on a mean distance of 1 µm. A slow signal strongly depending on the electric field is observed. For particle detection, only a small fraction of the signal from holes will then be readout, which will limit the detection efficiency.

Full depletion of the sensor is needed for an optimized signal from electrons but depletion of the sensor cannot be studied via standard C-V measurements as it is usually done with crystalline silicon sensors. Due to the high resistivity of the non-depleted i-layer, no variations of capacitance are observed changing V and therefore d. We propose a technique based on the photo-generation of electron-hole pairs close to the p-i interface with the 660 nm pulsed laser. Most of the readout charge depends on the integration of the current induced by electron motion. For a time $t > 3\times\tau_c$, this charge Qe can be obtained by integrating equation (5) and depends on the electron charge moving and on the ratio of the depleted thickness over the sensor thickness:

$$Qe = qNd / d_{tot} \quad (6); \qquad d = \sqrt{2\varepsilon_0\varepsilon_{asi} / (qN_{db}^{\ *})}\sqrt{V} \quad (7)$$

Tests have been carried out on a 20 µm thick sensor deposited on an aSiHtest chip. Structures connected to pre-amplifiers with 70 e^- rms noise and 25 ns peaking time have been characterized. The readout electronic peaking time is higher than $3\times\tau_c$ so that the measured output pulse maximum corresponds to the charge Qe readout. Evolution of Qe for varying detector biases is presented in Fig 8.

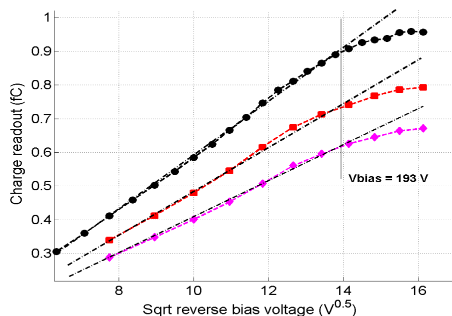

Fig 8. Charge created by a 3 ns FWHM 660 nm laser pulse as a function of the reverse voltage applied on the a-Si:H sensor. Results obtained on a 20 µm thick sensor deposited on an aSiHtest chip for 3 different laser amplitudes are shown.

Qe increases with the square root of the voltage, which is consistent with equations (6) and (7). The slope depends on qN and then increases for increasing amplitude of laser. Saturation starts to occur for a reverse voltage of ~ 193 V, which then corresponds to the depletion voltage, as the created charge saturates for $d = d_{tot}$. This method is successful in determining experimentally the a-Si:H sensor depletion. The density of ionized dangling bonds can also be extracted from this measurement and $N_{db}^{\ *} \sim 6.4\times10^{14}$ cm^{-3}. The extracted value is in agreement with the expected value of $N_{db}^{\ *} \sim 6\times10^{14}$ cm^{-3}.

C. Radiation detection with TFA detectors

Direct detection of charged particles and of soft X-rays have been carried out on a TFA detector based on a 15 µm thick sensor deposited on a MACROPAD circuit. Signals from the detector were readout on an oscilloscope in self-trigger mode. Signal pedestals and peak amplitudes were recorded via a Labview program. A maximum reverse bias of 145 V could be applied to the sensor, and the noise level of the readout electronics was measured equal to 40 e^- rms. The spectrum obtained with 5.9 keV X-rays from a Fe^{55} source is shown in Fig 9.

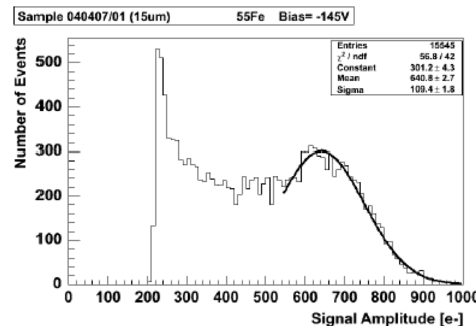

Fig 9. Spectrum of 5.9 keV X-rays from Fe^{55} source obtained on a 15 µm thick a-Si:H sensor deposited on a MACROPAD circuit, for a reverse bias of 145 V and a threshold of 200 e^-.

A broad peak is observed with a peak charge at about 650 e^- rms. The signal corresponds to charges induced by the transport of both electrons and holes. Fast construction of the signal induced by the electron drift has been demonstrated, but low and field dependent signal induced by holes has been observed. The total charge created by a particle or a photon in the a-Si:H sensor will depend on the location of creation of the electron-hole pairs. The signal corresponding to pairs created close to the p-i interface will be built principally by the electron drift and is expected to be complete. As pairs are created further into the depleted region, lower signal is created from electron drift and higher contribution from holes is expected. However, due to the low drift mobility of holes, only part of the signal from holes is readout. A mean energy of electron-hole pairs in a-Si:H of 4.8 to 6 eV [17] is considered. X-rays interacting close to the p-i interface induce a maximum signal and a total charge of 1000 to 1230 e^- is expected, while a maximum signal of about 900 to 1000 e^- is readout. X-rays creating pairs further into the sensor will induce a lower signal because of a lower collection of signal from holes, thus the peak has lower amplitude at about 650 e^-. No saturation of the peak charge was observed, as a peak charge of 510 e^- and of 582 e^- were readout for applied biases of 110 V and 130 V even though full depletion of the film is expected for biases higher than 110 V. This can be explained by a non full

depletion of the sensor and by the increase of the signal created by holes as the internal electric field is increased.

IV. CONCLUSION

TFA detectors based on n-i-p a-Si:H sensors with thickness from 15 µm to 32.6 µm and on 3 different integrated circuits have been developed.

Higher leakage currents have first been measured on TFA detectors in comparison to similar a-Si:H sensors deposited on a glass substrate. These high leakage currents prevent the full depletion of sensors with thicknesses up to 32.6 µm. However, fully depleted sensors with such thickness are needed for optimized detection efficiency, so that the reduction of the leakage current is a crucial parameter for the development of this technology. Leakage currents can be attributed to field enhanced thermal generation of charges by Poole-Frenkel mechanisms. The activation energy decreases for increasing bias voltage and equals ~ 0.42 eV for a 160 V reverse voltage applied to a 20 µm thick diode. High currents have been found originating from the pixel edges and corners. These additional currents are caused by the unevenness of the ASIC surface due to the passivation layer steps. We have shown that opening the passivation layers outside metal pads permits a reduction of the leakage current.

Signal induction and speed have been studied and a construction of signal from electron drift in a maximum time of 16.8 ns has been shown. The laser measurement technique permits to measure the full-depletion voltage which has been found to be ~ 193 V for a 20 µm thick sample. Full-depletion is required to obtain a maximum signal from electrons generated in the sensor depleted region. Hole mobility is field dependent and therefore the signal induced by hole motion in few tens of ns (which correspond to the pre-amplifier shaping time) strongly depends on the reverse voltage applied to the sensor and will not be complete.

Detection of 5.9 keV X-rays has been performed on a TFA detector with a 15 µm thick sensor. In order to optimize the detector efficiency for particle detection, thicker a-Si:H sensors fully depleted are needed. They would permit a higher interaction volume for charged particles and at the same time higher internal fields thus enhancing the detection efficiency. Radiation hardness of the developed detectors is a crucial parameter and is under study.

Instability of the sensor leakage current has been observed during the development and characterization of this novel technology. Moreover, long term stability has not been characterized and proven yet and is a crucial parameter under study. Finally, problems of yield of a-Si:H sensors deposited on ASIC have been observed and need further investigations.

ACKNOWLEDGMENT

The authors are glad to thank colleagues and collaborators for their important contribution and help in the work presented: W. Riegler for very useful discussions, C. Miazza and S. Dunand for the depositions of the a-Si:H sensors, D. Campos-Garcia and M. Fransen for their help and J. Morse and I. Snigireva for the EBIC measurements performed at the ESRF in Grenoble.

REFERENCES

[1] P. Jarron, G. Anelli, S. Commichau, M. Despeisse, G. Dissertori, C. Miazza, D. Moraes, A. Shah, G. Viertel, N. Wyrsch, Nucl. Instr. And Meth. In Phys. Res. A518 (2004) pp. 366-372.

[2] N. Wyrsch, S. Dunand, C. Miazza, A.Shah, G. Anelli, M. Despeisse, A.Garrigos, P. Jarron, J. Kaplon, D. Moraes, S.C. Commichau, G. Dissertori and G.M. Viertel, Physica Status Solidi (c), 2004, Vol. 1(5), pp. 1284-1291.

[3] N. Kishimoto, H. Amekura. N. Kishimoto, H. Amekura, K. Kono, C.G. Lee, Journal of nuclear materials, 258-263 (1998) 1908-1913

[4] J.R. Srour, G. J. Vendura, D. H. Lo, C.M.C. Toporow, M. Dooley, R.P. Nakano and E.E. King, IEEE Trans. On Nucl. Sc., vol. 45, no. 6, (1998), pp. 2624-2630.

[5] V. Perez Mendez et al., Nucl. Instr and Meth. A273, 127 (1988).

[6] A. Kolodziej. Opto-electronics review 12(1), 21-32 (2004).

[7] N. Wyrsch, C. Miazza, S. Dunand, A. Shah, N. Blanc, R. Kaufmann, L. Cavalier,G. Anelli, M. Despeisse, P. Jarron, D. Moraes, A. G. Sirvent, G. Dissertori, G. Viertel. Proceedings of the MRS Spring Meeting, San Francisco, April 2003, MRS Vol. 762, pp. 205-210.

[8] J. Dubeau, T. Pochet, L. A. Hamel, B. Equer, A. Karar. Nucl. Instr. And Meth. In Phys. Res. B, 1991, Vol. 54, pp. 458-471.

[9] C. Hordequin, A. Brambilla, P. Bergonzo, F. Foulon. Nucl. Instr. And Meth. In Phys. Res. A, 2001, Vol. 456, pp. 284-289.

[10] G. Anelli, K. Borer, L. Casagrande, M. Despeisse, P. Jarron, N. Pelloux and S. Saramad. Nucl. Instr. And Meth. In Phys. Res. A **512** (2003), p. 117.

[11] D. Moraes, G. Anelli, M. Despeisse, P. Jarron, J. Kaplon, A.Garrigos Sirvent, N. Wyrsch, C. Miazza, S. Dunand, A. Shah, G. Dissertori, G. Viertel. J. Non-Cryst. Solids 338-340 (2004), pp. 729-731.

[12] F. Meillaud, A. Shah, C. Droz, E. Vallat-Sauvain, C. Miazza, to be published in Solar Energy and Materials and Solar Cells.

[13] J. B. Chévrier and B. Equer, J. Appl. Phys. 76 (11), 1994, pp. 7415-7422.

[14] M. Despeisse, G. Anelli, S. Commichau, G. Dissertori, A. Garrigos, P. Jarron, C. Miazza, D. Moraes, A. Shah, N. Wyrsch, G. Viertel. Nucl. Instr. And Meth. In Phys. Res. A518 (2004), pp. 357-361.

[15] W. Riegler, Nucl. Inst. And Meth. In Phys. Res. A, 2004, Vol. 535, pp. 287-293.

[16] Q. Gu, E.A. Schiff, J-B. Chévrier and B. Equer. Phys. Rev. B, 1995, Vol. 52, n° 8, pp. 5695-5707.

[17] S. Najar, B. Equer and N. Lakhoua. J. Appl. Phys., 1991, Vol. 69, No. 7, pp. 3975-3985.